Role of mast cells in wound healing process after glass - fiber composite implant in rats

L. F. Rodella [a, #], Rita Rezzani [a, *, #], Barbara Buffoli [a], Francesca Bonomini [a], Sandra Tengattini [a], Laura Laffranchi [b], C. Paganelli [b], P. L. Sapelli [b], Rossella Bianchi [a]

[a] Division of Human Anatomy, Department of Biomedical Sciences and Biotechnologies, University of Brescia, BS, Italy
[b] Dental School, University of Brescia, BS, Italy

Abstract

Glass-fiber composites are frequently used in dentistry. In order to evaluate their biocompatibility we tested, in an experimental model "*in vivo*", their tissue response pointing our attention on presence of mast cells (MCs) and fibrotic process. Sprague Dawley rats were used for the experimental design. The fibers were introduced in a subcutaneous pocket along the middle dorsal line between the two scapulas for 7, 14 or 21 days. At the end of the treatments the skins were excised and then processed for Toluidine Blue, to determine the presence of MCs, and Picrosirius Red staining, to evaluate the presence of fibrotic tissue. Our preliminary results showed and increase of both MC number and deposition of collagen type I, which characterized the fibrotic tissue. So, subsequent aims of our study were to evaluate the role played by MCs in tissue fibrosis and to give a possible explanation regarding the mechanisms that were responsible of biological response observed, through the analyses of some proteins, such as metalloproteinase-2 (MMP-2), its inhibitor (TIMP-2) and transforming growth factor-β (TGF-β). Our data confirmed the involvement of TGF-β, released by MCs, in the disruption of the equilibrium between MMP-2 and TIMP-2 that were implicated in the enhancement of fibrosis. In summary, this study demonstrate that this type of materials induced an inflammatory response at the site of implant and help to clarify what type of mechanism and which proteins are involved in this biological response. Nevertheless, more extensive investigations are in progress to better evaluate the inflammatory process.

Keywords: biocompatibility • mast cells • fibrosis • dentistry

Introduction

The concept of biocompatibility is based on the interactions between a material and a biological environment. The failure of a biomaterial, in a clinical situation, to display good biocompatibility is often revealed by a breakdown in the desired material properties or an unsatisfactory biological response. The most important aspect of biocompatibility, for the performance of the material, is the local response, as this usually provides a clinical indication of a biocompatibility deficiency [1]. Analysis of the local tissue response to a biomaterial has long been recognized to play an important role in biocompatibility testing. The normal wound-healing response is a

The authors share the first authorship
* Correspondence to: Prof. Rita REZZANI
Division of Human Anatomy, Department of Biomedical Sciences and Biotechnologies, University of Brescia, V.le Europa 11, 25123, Brescia, Italy.
Tel.: +39 030 3717483
Fax: +39 030 3717486
E-mail: rezzani@med.unibs.it

dynamic phenomenon, in which cells and their products interact to repair damaged tissue. If an implant is present in the tissue, this sequence of events is disrupted to varying degrees, resulting in a visible change in tissue morphology. Many types of cells are involved in normal wound healing, including inflammatory cells that are the predominant components of cell/polymer interactions and, in particular, macrophage activation induces the cells to further differentiate, phagocytose or to the surrounding environment, being an important macrophage property their ability to recognize foreign surfaces [2, 3]. Moreover, wound healing in the presence of biomaterial may induce a more complex reaction involving different types of cells that may trigger an array of iatrogenic effects including inflammation, fibrosis, coagulation and infection [4]. In view of the inert and non-toxic nature of most biomaterials, it is puzzling that tissue contact implants very often acquire an extensive overlay of phagocytic cells. These phagocytes have been implicated in a number of subsequent adverse effects such as osteolytic changes around joint implants [5], degradation of biomaterial implants [6] and fibrosis surrounding prostheses [7] and many other types of implants [8, 9]. It has been demonstrated that materials, such as standardized implants of calcium hydroxide, glass ionomer cement and allows for ceramic crowns and for removable prostheses, surgically introduced into Wistar rats' back bone and along the middle dorsal line between the two scapulas respectively, triggered various inflammatory responses. These latters were responsible to interstitial fibrosis and to increased number of mast cells (MCs) [10, 11]. Moreover, it has been shown that the presence and the disposition of fibrous tissue around implants of dental materials are indicative to tissue response. So, the biocompatibility of a material is inversely related to the amount of fibrosis developed around it [12].

In attempting to well define the influence of biomaterial presence on the normal would-healing response and to assessment the degree of local tissue response to the implants, we considered the polymer-fiber composites that reached almost all disciplines of dentistry [13], and that are, in particular, used for removable prostodontics [14]. In fact, in the last ten years, different fiber products composed predominantly of glass fibers have been introduced since they have good resistance to traction and tearing, high modulus and dimensional sta-

bility [15]. To our knowledge, there are no data about their tissue response, so the objectives of this work are threefold: **1)** to test in an experimental model "*in vivo*" the biocompatibility of the glass-fiber composites (FRCs), using the two above reported points, the involvement of MCs and the presence of fibrotic tissue near the implant; **2)** to evaluate the role played by MCs in tissue fibrosis; **3)** to give a possible explanation regarding the mechanisms that are responsible of biological response to biomaterials since, when it is aberrant, many pathological conditions can born or be exacerbated. So, we focused our attention on the role of some proteins, such as matrix metalloproteinase-2 (MMP-2), its tissue inhibitor (TIMP-2) and transforming growth factor-β (TGF-β). They are involved in many biological processes as well as normal tissue remodelling, embryogenesis, wound healing and angiogenesis. In particular, it is reported that TGF-β facilitate collagen production, as well as the expression of MMPs, which are responsible for tissue breakdown [16]. So, disruption of the equilibrium between these proteins has been shown to induce an increased and continuous deposition of extracellular matrix [17]. Moreover, the alteration of this balance results in serious diseases such as fibrosis, arthritis, and tumour growth [18].

Materials and methods

Animal and experimental design

60 adult male Sprague Dawley rats weighing 150–200g were obtained from Harlan Laboratories, Italy. They were housed in individual sterile cages with food and water ad libitum; the animal houses were kept at a constant temperature and humidity with 12 h alternating dark/light cycle. All the experiments were performed minimizing animal suffering according to the Italian Law on the protection of laboratory animals, as well as with Ethical Committee Regulations; all procedures were approved by Italian Ministry of Health.

After an adaptation period of two weeks, the rats were randomly divided into two main groups constituted by three subgroups (n = 10) for each one. Group 1a-b-c (control groups): the animals were sham operated respectively for 7, 14 and 21 days. Group 2a-b-c (experimental groups): the animals were implanted in subcutaneous pockets with

FRCs (Stick®Net, StickTech, Turku, Finland) and treated respectively for 7, 14 and 21 days. These cast specimens have a square shape of 1 cm^2 in size and a rough surface (it has not been smoothed after polymerization). The exact site of implantation is in a subcutaneous pocket along the middle dorsal line between the two scapulas as previously reported for different implanted biomaterials by Rezzani *et al.* [11]. At the end of the treatments, the animals were killed and the skin around implant was excised.

Preparation of FRC specimens

The FRC examined in this study was glass fiber (Stick®Net, StickTech, Turku, Finland). The fibers was impregnated with a light-polymerized resin (StickTech, Turku, Finland) and polymerized with a light-curing unit (Optilux 501, Sds Kerr, Danbury, CT) for 40 seconds. The wavelength of the unit was between 380 and 520 nm and the light intensity was 700 mW/cm^2 verified with the light-curing unit's internal radiometer. At the end of polymerization, the specimens were refined but not smoothed. For our aim, pieces, approximately, 10 x 10 mm in size and 1 mm in thickness, were cut with a surgical knife.

Histopathological analysis

Skin samples were, first of all, washed in phosphate buffer saline (PBS) 0.1M (pH 7.4), then were fixed in 10% buffered formalin, embedded in paraffin according to standard procedures and serially sectioned at 5 μm by microtome. For histopathological evaluation, these sections were deparaffined, rehydrated, immersed in water and, finally, stained with: - Toluidine Blue, for identification of MCs and visualization of granules present in these cells; - Picrosirius Red for assessing the presence of fibrosis.

For the toluidine blue staining, the samples have been treated according to Rezzani *et al.* [11].

The quantitative evaluation of MCs was estimated in a blinder fashion in 10 samples for both control and experimental groups at a final magnification of 20 x. The number was calculated for arbitrary areas, measuring 10 fields with the same area for each sample and, successively, statistically studied.

For Picrosirius Red method, the sections were stained for 30 minutes with phosphomolybdic acid 0.1%, washed in water and then immersed in Picrosirius Red (Sirius Red 0.1% in picric acid) for 60 minutes at room temperature (RT). Successively, the sections were washed in water

and then rapidly dehydrated, cleared in xylene and mounted. Collagen fibers were detected both by light and polarized light microscopy (Olympus; Milan, Italy). Under polarized light microscopy, type I collagen fibers were stained from orange to red, whereas the type III collagen fibers appeared green [19]. The quantitative evaluation of collagen type was evaluated as percentage of orange/red fibers in 10 samples of both control and experimental groups. 10 fields were chosen for each sample, in which the percentage of area injured, using an optical polarized light microscope at a final magnification of 10 x, was counted. The percentage of collagen type was observed in a blind fashion, calculated in arbitrary areas and, successively, statistically studied.

Immmunohistochemical analysis

Briefly, the skin sections were fixed in 10% buffered formalin and embedding in paraffin. Before immunodetection, they were deparaffined and subjected to antigen retrieval in 0.05M sodium citrate buffer (pH 6.0) in a microwave oven (2 cycles of 5 minutes at 650W and 1 cycle of 3 minutes at 400W) according to Boon [20]. Endogenous peroxidase activity was blocked by incubation with a solution of 3% hydrogen peroxide in methanol for 30 minutes (RT). Sections were then incubated with appropriated normal serum (diluted 1:5 Dakopatts, Italy) for 60 minutes, and serially treated overnight (ON) at 4°C with MMP-2 (goat polyclonal, diluted 1:50, Santa Cruz, USA) and TIMP-2 (mouse monoclonal, dilute 1:100, Chemicon, USA) antibodies. The sections were washed in Tris buffer solution (TBS) 0.1M (pH 7.4) and sequentially incubated with proper biotinylated secondary antibody (diluted 1:50 Dakopatts, Italy), washed again and incubated for 1 hr (RT) using an avidin-biotin horseradish peroxidase complex according to the manufacturer's instructions (ABC kit, Dakopatts, Italy). Finally, peroxidase activity was demonstrated using a solution of 0.05% 3,3-diaminobenzidine tetrahydrochloride and 0.33% hydrogen peroxide. All sections were counterstained with haematoxylin, dehydrated and mounted. Control reactions were performed in the absence of the primary antibodies and with isotype-matched irrelevant rat IgGs as negative control.

For semiquantitative analysis, the degree of MMP-2 and TIMP-2 staining was evaluated by an observer blinded and was graded as: (–) when there was no signal, (+/-) when the staining was very weak, (+) when the staining was weak, (++) when it was moderately positive and (+++) when it was strong.

Immunoblotting analysis for MMP-2, TIMP-2 and TGF-β proteins.

The tissue was homogenised in a buffer system as described below: 15 mg of frozen cutaneous rat tissue was minced and extracted in 300 µl 2% sodium dodecyl-sulfate (SDS)/PBS solution and incubate ON at 4°C. The homogenate was centrifugated with 12000 rpm at 4°C for 15 minutes, and the supernatants were processed using immunoblotting analysis, gelatin zymography or reverse zymography. Protein concentration was assessed using Albumin Standards (Pierce, Illinois) according to the manufacturer's instruction. 10 µg of the samples were analysed by 10% SDS-PAGE and electro-transferred to a nitro-cellulose membrane (pore size 0.45 µm; BioRad) by wet blotting (100V for 1 hr). The membrane was blocked with 5% non-fat dry milk in Tris-buffered saline Tween-20 (TTBS) at 4°C. After washing with TTBS, proteins were exposed overnight at 4°C to goat polyclonal anti-MMP-2 and mouse monoclonal anti-TIMP-2 and anti TGF-β. These were detected using a proper biotinylated secondary antibodies (Dakopatts) and an avidin–peroxidase complex according to the manufacturer's instructions (ABC kit, Dakopatts), with a solution of 0.05% DAB (3.3-diamino-benzedine tetrahydrochloride) and 0.03% hydrogen peroxide. For the quantitative analyses, the bands were evaluated as integrated optical density (IOD), using Gel Pro 3.1 software, and the data obtained were statistically studied.

Zymographic and reverse zymographic analysis for MMP-2 and TIMP-2 protein respectively

For zymography, MMP-2 activity was detected according to Rawdanowicz *et al.* [21] with minor modifications. 10 µg of the samples were loaded onto 10% SDS-polyacrilamide gels containing 1 mg/ml bovine gelatin under non-reducing conditions. Following electrophoreses, the gel was washed twice with 2.5% Triton-X-100 solution for 15 minutes each, rinsed with incubation buffer (50mM TRIS HCl, pH 8.0; 5mM $CaCl_2$) and incubated in the same buffer at 37°C ON. The gel was stained with Comassie Blue R250 and destained in water. Gelatinase was detected as white bands against a blue blackground.

For reverse zymography, TIMP-2 was measured according to Olivier *et al.* [22]. The standard separating gel was prepared with 2.25 mg/ml porcine gelatine, 4 ml H_2O, 3.3 ml acrilamide mix, 2.5 ml Tris–HCl pH 8.8 1.5

mol, 0.1 ml SDS 1%, 0.1 ml APS 1%, 0.004 ml TEMED and 160 ng/ml pro-gelatinase A. A standard stacking gel was used. After electrophoresis, gels were agitated in two washes (both 30 minutes duration) of 2.5% Triton X-100 to remove the SDS and restore enzyme activity for incubation. Gels were incubated for 16 hrs at 37°C in 50 µl of 50 mmol Tris–HCl (20 mol NaCl, 50 mmol Tris, 5 mmol $CaCl_2$, pH 7.6; all chemicals from Sigma Chemical Co., St. Louis, MO, USA). Finally gels were stained with Comassie Blue R-250 and then destained in water.

For the quantitative analyses, the bands were evaluated as integrated optical density (IOD), using Gel Pro 3.1 software, and the data obtained were statistically studied.

Statistical analysis

The results for all analyses are presented as means ± SEM and the statistical significance of differences among experimental groups was estimated using the ANOVA test corrected by Bonferroni, with $P < 0.05$ considered as significant.

Results

The skin of control groups at both 7, 14 and 21 days did not show any differences for all analyses; so, we decided to consider them without distinction.

Histopathological study of the skin

The skin of all control groups showed a normal morphology without signs of alterations. Instead, we observed time-dependent changes in the tissue of experimental groups. These alterations were noted in the dermis and regarded the presence of MCs and the appearance of fibrosis. As shown in Fig. 1 MCs were not present in control groups but they were found already 7 (group 2a) days after the treatment. Moreover, most of them were degranulated near the site of implant (Fig. 1D).

The appearance of fibrosis was visible at 7 days after the implant (group 2a) and this enhancement was very high 21 days after (group 2c) (Fig. 2). In particular, control groups showed mainly collagen type III, that is constitutively present and visualized in green colour (Fig. 2A), whereas the fibrosis has been clearly seen as deposition of collagen type
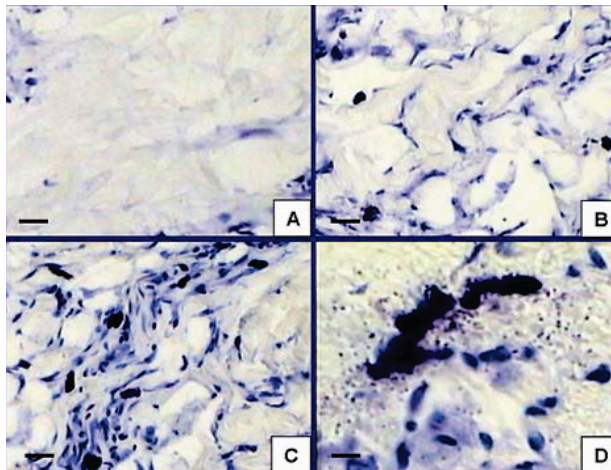
Fig. 1 Photomicrographs showing Toluidine Blue staining of rat skin from control (**A**) and experimental groups at 7 (**B**) and 21days (**C**) from implant placement (Bar 20 μm). Photomicrograph **D** shows degranulating mast cells near the implant (Bar 8 μm).

I visualized in orange/red colour under polarized microscope (Figs 2B, 2C).

All quantitative data of MC number and percentage of fibrosis are reported in Fig.3. We observed a significant MC increase in experimental groups respect to control already 7 days after implant (group 2a); on the contrary, we observed a statistically significant only 21 days after the beginning of treatment (group 2c).

Immunohistochemistry and immunoblotting analysis of MMP-2 and TIMP-2 proteins

In the fibroblasts of dermis, MMP-2 immunostaining was very weak in control, whereas it appeared to increase ranging from 7 to 21 days after the treatment (Fig. 4A). Instead, TIMP-2 immunohistochemistry, in the same cells, was moderate in control and completely negative 21 days from implant placement (group 2c) (Fig. 4B). Moreover, as shown in Fig. 4C, MCs were negative to MMP-2 and TIMP-2 already at 7 days after the treatment (group 2a) and they remain negative also at the end of the treatment.

Negative control for immunohistochemistry did not show MMP-2 or TIMP-2 expression in skin from both control and experimental groups.

All semiquantitative immunostaining data are reported in Table 1.

Immunoblotting analysis for both proteins confirmed the immunohistochemical data (Figs 5A, 5B). The densitometric analysis of MMP-2 and TIMP-2 levels are reported in Fig. 5C.

Zymographic and reverse zymographic analysis for MMP-2 and TIMP-2 proteins respectively

The zymographic analysis revealed basal levels of MMP-2 activity in control groups and an increased amount of MMP-2 activity in experimental groups. In particular, very high levels of MMP-2 were found 21 days after surgery (group 2c) (Fig. 6A). This analysis allowed to visualize not only activated MMP-2 but also the activity of its precursor form, pro-MMP-2. On the contrary, the reverse zymographic analysis revealed highest level of TIMP-2 activity in control groups and very low levels 21 days after surgery (group 2c) (Fig. 6B). The densitometric readings of MMP-2 and TIMP-2 activity are shown respectively in Figs. 6C and 6D.
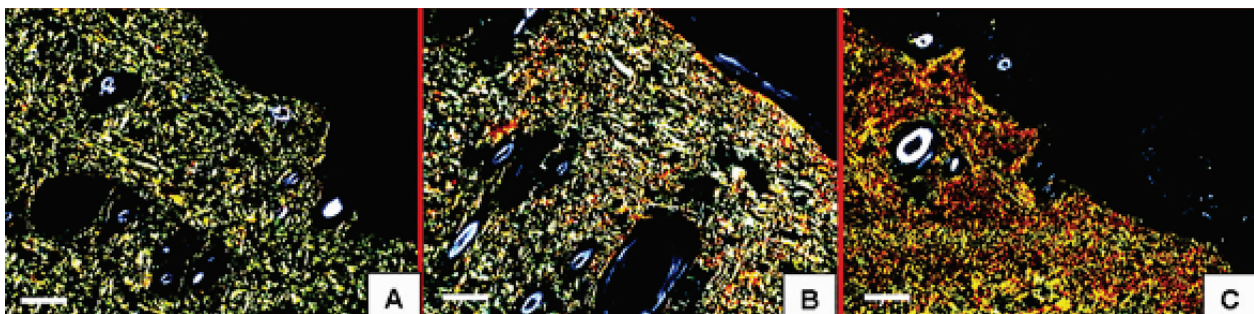
Fig. 2 Photomicrographs showing Sirius red staining, under polarized light microscope, of rat skin from control (**A**) and experimental groups at 7 (**B**) and 21 (**C**) days from implant placement (Bar 80 μm).

Immunoblotting analysis of TGF-β protein

Immunoblotting analysis of TGF-β showed a significant increase of this protein in the experimental groups respect to control. This enhancement was well evident and statistically significant 7 days after surgery (group 2c); its levels remained high also 14 and 21 days after implant placement (respectively, group 2b and 2c) (Fig. 7A). The densitometric analysis of TGF-β levels are reported in Fig. 7B.

Discussion

In the present study we assessed the biocompatibility of FRCs, which are generally used in dentistry field and, in particular, for removable prostodontics. Our results showed that the biocompatibility of this biomaterial is no good since it interferes with normal biological metabolism disrupting the normal wound-healing processes and inducing a different tissue response. In fact, the tissue response in the rat skin is characterized by: **1**) increase in the number of MCs with extensive degranulation, which was significant respect to control groups only 7 days after surgery and **2**) an enhancement of fibrotic process which resulted statistically significant 21 days after treatment only. These data are in agreement with several lines of evidence suggesting that MCs are involved in fibrotic process and tissue remodeling [23, 24].

MCs may exert bi-directional effect on matrix turnover contributing: **1**) indirectly, inducing the synthesis of certain types of mediators from secretory granules that have fibrogenic effects; **2**) directly, through their ability to produce extracellular matrix glicoproteins.
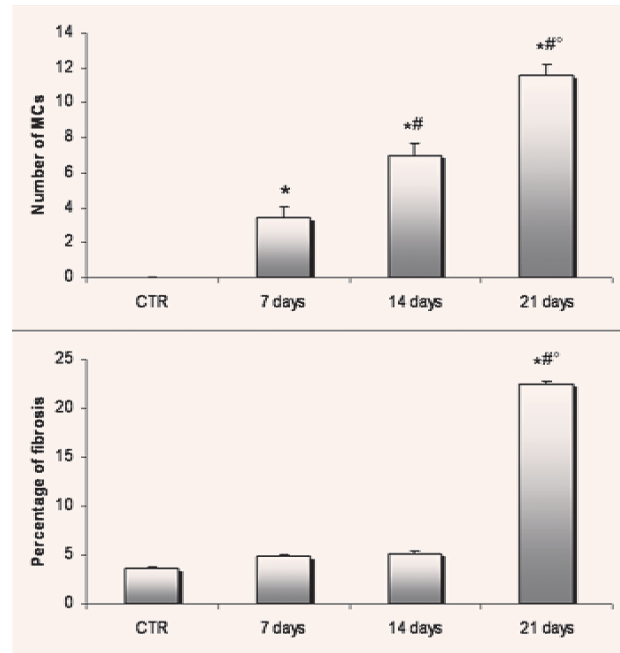
Fig. 3 (**A**) Quantitative analysis of the number of MCs present in rat skin of control and experimental groups. (**B**) Quantitative analysis of collagen content in rat skin of control and experimental groups. Data are expressed as means + SEM. * P < 0.05 *vs.* control; # P < 0.05 *vs.* 7 days after the implant; ° P < 0.05 *vs.* 14 days from implant placement.

Regarding the first effect, the degranulation of MCs have been documented in fibrotic processes "*in vivo*" determining the liberation of several mediators such as TGF-β that facilitate collagen production, as well as the expression of MMP enzymes, which are responsible for tissue breakdown [25]. As illustrated in Fig. 8, our study provided support for the concept above reported suggesting that TGF-β, produced by MCs, induces
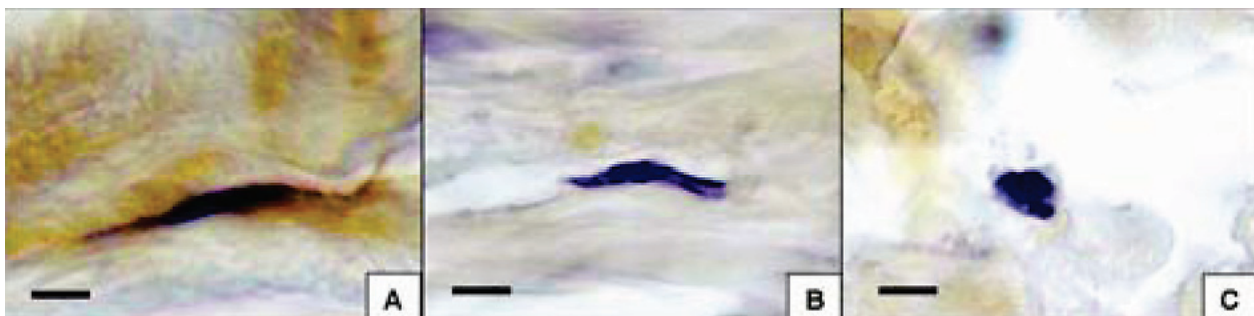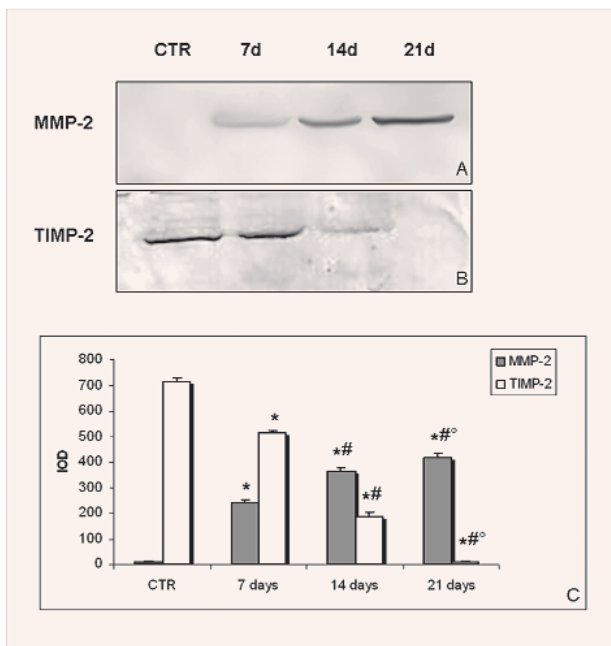

Fig. 4 Immunohistochemical localization for MMP-2 and for TIMP-2 in fibroblast of skin from experimental group (21 days after implant placement) (**A**, **B**) and in mast cells (**C**) (Bar 8 μm).

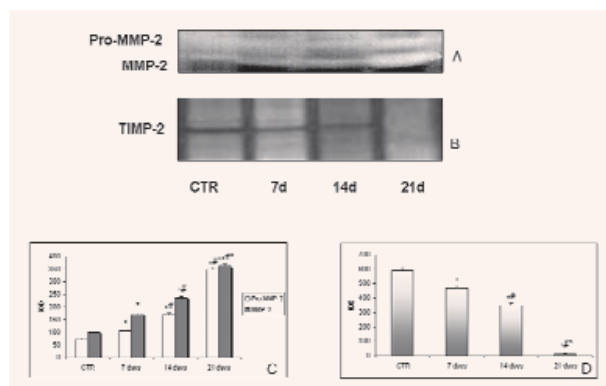**Table 1** Semiquantitative analysis of MMP-2 and TIMP-2 expression

Groups	MMP-2	TIMP-2
Controls	+/-	++
7 days	+	+
14 days	++	-
21 days	+++	-

For semiquantitative analysis, the degree of MMP-2 and TIMP-2 staining was evaluated by an observer blinded and was graded as: (-) when there was no signal, (+/-) when the staining was very weak, (+) when the staining was weak, (++) when it was moderately positive and (+++) when it was strong.

MMP-2 in fibroblasts and contributed to the enhancement of fibrotic process. Because many fibrogenic MC factors are also produced by other

Fig. 6 (**A**) Representative gelatin of MMP-2 zymographic analysis of protein extracts obtained from skin of control (lane 1) and of rats at 7 (lane 2), 14 (lane 3) and 21 (lane 4) days after implant placement. (**B**) Representative gelatin of TIMP-2 zymographic-reverse analysis of protein extracts obtained from skin of control (lane 1) and of rats at 7 (lane 2), 14 (lane 3) and 21 (lane 4) days after implant placement. (**C-D**) Quantitative analyses of MMP-2 zymography and TIMP-2 reverse-zymography are presented in bar graphs; representative blots with integrated optical density (IOD) readings are expressed as arbitrary units. * $P < 0.05$ *vs.* control; [#] $P < 0.05$ *vs.* 7 days after the implant placement; ° $P < 0.05$ *vs* 14 days after the implant placement.

Fig. 5 (**A**, **B**) Western blot analysis of MMP-2 (**A**) and TIMP-2 (**B**) in rat skin from control and experimental groups at 7, 14 and 21 days from implant placement. (**C**) Quantitative analyses of MMP-2 and TIMP-2 expressions are presented in bar graphs; representative blots with integrated optical density (IOD) readings are expressed as arbitrary units. * $P < 0.05$ *vs.* control; [#] $P < 0.05$ *vs.* 7 days after the implant placement; ° $P < 0.05$ *vs.* 14 days after the implant placement.
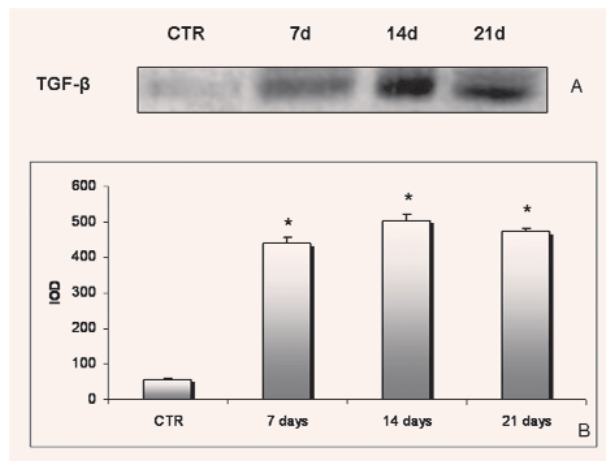
Fig. 7 (**A**) Western blot analysis of TGF-β in rat skin from control and experimental groups at 7, 14 and 21 days after implant placement. (**B**) Quantitative analyses of TGF-β expression are presented in bar graphs; representative blots with integrated optical density (IOD) readings are expressed as arbitrary units. *$P < 0.05$ *vs.* control.

952

Fig. 8 Schematic model of mast cell bio-directional effect on matrix turnover. The MCs activation induces: **1**) TGF-β liberation from secretory granules that determines MMP-2 production in fibroblasts (indirect mechanism); **2**) TNF-α secretion with degranulation that determines, by a feed-back mechanism, the MMP-2 synthesis in the same cells (direct mechanism). Green arrow indicates the hypothesis supported by our data, whereas red arrows indicate the mechanism excluded.
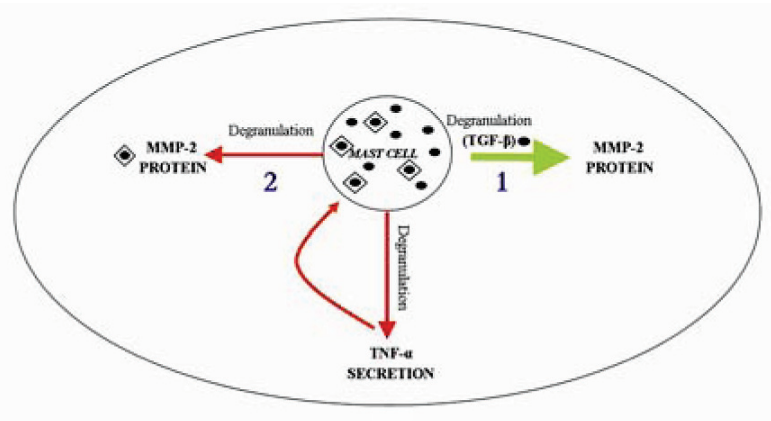
cell types involved in fibrotic process, such as macrophages, it is difficult to define the precise role that MCs play in this process. One model that offers the potential for further investigation is the genetically MC deficient W/Wc mouse [26]. If these animals show an impaired fibrogenic response after the treatment that is not seen in the wild-type littermates with normal MC numbers and this is reversible after reconstruction with wild-type bone marrow cells, then an important role for MCs in skin fibrosis is established. It has already been demonstrated in an animal model that cutaneous fibrosis may be inhibited by MC stabilizing agents [27] and that in tight-skin lesions MC are involved/recruited and their proliferation and activation lead to augmentation of fibrosis [28].

Regarding the second effect played by MCs on matrix turnover, there are data supporting the idea that the MC activation induces secretion of Tumor Necrosis Factor-α (TNF-α) which, released from these cells, by a feed-back mechanism, activates "*in vitro*" the zymogen forms of matrix metalloproteinases and protocollagenase [29]. Our data are not in agreement with these results showing that MMP-2 was not present in secretory granules of MCs during all treatment. So, we suggest that, since MMP-2 is not produced by MCs, and we found an increase of TGF-β expression in skin, MCs could act by an indirect mechanism on fibrotic processes.

Another interesting point of this study regards the variation of TIMP-2 expression. We showed that MCs were negative to this protein during all treatment but it was present in fibroblast cytoplasm of control groups. Western blotting analysis showed a decrease of TIMP-2 protein 14 and 21 days after the implant. So, these results could suggest that TIMP-2 alterations were linked to fibroblast cytoplasm only since there is not any presence of this protein in MCs. Moreover, TIMP-2 decrease could be related to MMP-2 alterations and its variation should be a compensatory mechanism against the excessive accumulation of collagen as previously demonstrated [30]. In particular, MMP-2 increase in cytoplasm of fibroblasts could induce a decrease of its inhibitor.

Even if it should be represent an important point for the future rational design of biocompatible biomaterials, more extensive investigations are in progress to better characterize the inflammatory process and the evaluation of the involvement of other different cell types, such as macrophages and lymphocyte subpopulations.

Acknowledgements

References

1. **Ogasawara T, Yoshimine Y, Yamamoto M, Akamine A.** Biocompatibility of an experimental glass-ionomer cement sealer in rat mandibular bone. *Oral Surg Oral Med Oral Pathol Oral Radiol Endod*. 2003; 96: 458–65.
2. **Bosetti M, Ottani V, Kozel D, Raspanti M, De Pasquale V, Ruggeri A, Cannas M.** Structural and functional macrophages alterations by ceramics of different composition. *Biomaterials* 1999; 20: 363–70.

3. **de Oliveira Mendes ST, Ribeiro Sobrinho AP, de Carvalho AT, de Souza Côrtes MI, Vieira LQ.** *In vitro* evaluation of the cytotoxicity of two root canal sealers on macrophage activity. *J Endod*. 2003; 29: 95–9.

4. **Tang L, Jennings TA, Eaton JW.** Mast cells mediate acute inflammatory responses to implanted biomaterials. *Proc Natl Acad Sci*. 1998; 95: 8841–6.

5. **Hallab NJ, Cunningham BW, Jacobs JJ.** Spinal implant debris-induced osteolysis. *Spine* 2003; 28: S125–38.

6. **Mabilleau G, Moreau MF, Filmon R, Baslé MF, Chappard D.** Biodegradability of poly (2-hydroxyethyl methacrylate) in the presence of the J774.2 macrophage cell line. *Biomaterials* 2004; 25: 5155–62.

7. **Tang L, Jiang W, Welty SE.** The participation of P- and E-selectins on biomaterial-mediated tissue responses. *J Biomed Mater Res*. 2002; 62: 471–7.

8. **Busuttil SJ, Plopis VA, Castellino FJ, Tang L, Eaton JW, Plow EF.** A central role for plasminogen in the inflammatory response to biomaterials. *J Thromb Haemost*. 2004; 2: 1798–805.

9. **Suska F, Gretzer C, Esposito M, Emanuelsson L, Wennerberg A, Tengvall P, Thomsen P.** *In vivo* cytokine secretion and NF-kappaB activation around titanium and copper implants. *Biomaterials* 2005; 26: 519–27.

10. **de Oliveira Mussel RL, De Sa Silva E, Monte Alto Costa A, Mandarim-De-Lacerda CA.** Mast cells in tissue response to dentistry materials: an adhesive resin, a calcium hydroxide and a glass ionomer cement. *J Cell Mol Med*. 2003; 7: 171–8.

11. **Rezzani R, Rodella L, Tartaglia GM, Paganelli C, Sapelli P, Bianchi R.** Mast cells and the inflammatory response to different implanted biomaterials. *Arch Histol Cytol*. 2004; 67: 211–7.

12. **Costa CA, Teixeira HM, do Nascimento AB, Hebling J.** Biocompatibility of two current adhesive resins. *J Endod*. 2000; 26: 512–6.

13. **Vallittu PK.** Survival rates of resin-bonded, glass fiber-reinforced composite fixed partial dentures with a mean follow-up of 42 months: a pilot study. *J Prosthet Dent*. 2004; 91: 241–6.

14. **Vallittu PK.** Compositional and weave pattern analyses of glass fibers in dental polymer fiber composites. *J Prosthodont*. 1998; 7: 170–6.

15. **Bayraktar G, Duran O, Bural C, Guvener B.** Effects of water storage of E-glass fiber reinforced denture base polymers on residual methyl methacrylate content. *J Biomed Mater Res B Appl Biomater*. 2004; 70: 161–6.

16. **Manabe I, Shindo T, Nagai R.** Gene expression in fibroblasts and fibrosis. Involvement in cardiac hypertrophy. *Circ Res.* 2002; 91: 1103–13.

17. **Tilakaratne WM, Klinikowski MF, Saku T, Peters TJ, Warnakulasuriya S.** Oral submucous fobrosis: review on aetiology and pathogenesis. *Oral Oncol*. 2005; Epub ahead of print.

18. **Hamacher S, Matern S, Roeb E.** Extracellular matrix from basic research to clinical significance. An overview with special consideration of matrix metalloproteinases. *Dtsch Med Wochenschr*. 2004; 129: 1976–80.

19. **Zhang H, Sun L, Wang W, Ma X.** Quantitative analysis of fibrosis formation on the microcapsule surface with the use of picro-sirius red staining, polarized light microscopy, and digital image analysis. *J Biomed Mater Res A*. 2006; 76: 120–5.

20. **Boon ME.** Microwave-antigen retrieval: the importance of pH of the retrieval solution for MIB-1 staining. *Eur J Morphol*. 1996; 34: 375–9.

21. **Rawdanowicz TJ, Hampton AL, Nagase H, Wooley DE, Salamonsen LA.** Matrix metalloproteinase production by cultured human endometrial stromal cells: identification of interstitial collagenase, gelatinase-A, gelatinase-B and stromelysin-1 and their differential regulation by interleukin-1 alpha and tumor necrosis factor-alpha. *J Clin Endocrinol Metab*. 1994; 79: 530–6.

22. **Oliver GW, Leferson JD, Stetler-Stevenson WG, Kleiner DE.** Quantitative reverse zymography: analysis of pictogram amounts of metalloproteinase inhibitors using gelatinase A and B reverse zymograms. *Anal Biochem*. 1997; 244: 161–6.

23. **Krishnaswamy G, Kelley J, Johnson D, Youngberg G, Stone W, Huang SK, Bieber J, Chi DS.** The human mast cell: functions in physiology and disease. *Front Biosci*. 2001; 6: D1109–27.

24. **Mekori YA.** The mastocyte: the "other" inflammatory cell in immunopathogenesis. *J Allergy Clin Immunol*. 2004; 114: 52–7.

25. **Stawowy P, Maegeta C, Kallisch H, Seidah NG, Chrétien M, Fleck E, Graf K.** Regulation of matrix metalloproteinase MT1-MMP/MMP-2 in cardiac fibroblasts by TGF-β1 involves furin-convertase. *Cardiovasc Res*. 2004; 63: 87–97.

26. **Kitamura Y, Go S, Hatnaka S.** Decrease of mast cells in W/Wv mice and their increase by bone marrow traspalntation. *Blood* 1978; 52: 447–52.

27. **Walker MA, Harley RA, Leroy EC.** Inhibition of fibrosis in TSK mice by blocking mast cell degranulation. *J Rheumatol.* 1987; 14: 299–301.

28. **Everett ET, Pablos JL, Harley RA, Leroy EC, Norris JS.** The role of mast cells in the development of skin fibrosis in tight-skin mutant mice. *Comp Biochem Physiol A Physiol.* 1995; 110: 159–65.

29. **Baram D, Vaday GG, Salamon P, Drucker I, Hershkoviz R, Mekory YA.** Human mast cells release metalloproteinase-9 on contact with activated T cells: juxtacrine regulation by TNF-alpha. *J Immunol*. 2001; 167: 4008–16.

30. **Rezzani R, Giugno L, Buffoli B, Bonomini F, BianchiR.** The protective effect of caffeic acid phenethyl ester against cyclosporine A-induced cardiotoxicity in rats. *Toxicology*. 2005; 212: 155–64.